Nat Hazards (2009) 49:1–24
DOI 10.1007/s11069-008-9274-y

ORIGINAL PAPER

Spatial and temporal pattern of precipitation and drought in Gansu Province, Northwest China

Luxin Zhai · Qi Feng

Received: 22 August 2007 / Accepted: 15 July 2008 / Published online: 27 August 2008

Abstract Drought is one of the most harmful natural hazards in Gansu Province in Northwest China. The changes of precipitation affect the severity of drought. In order to recognize the trend of precipitation and understand the effect of rainfall change on water resources management and drought severity, Mann–Kendall test was used. Standardized Precipitation Index (SPI) was calculated to reconstruct the drought at different time scales and analyze the frequency of drought occurrence in the recent 50 years. The results show that the SPI is applicable in Gansu Province. The number of severe droughts differs among regions: it is more obvious as a 3-month drought in the Yellow River Basin and the Yangtze River Basin than in the Inland River Basin, and other droughts at 6-, 9-, and 12-month time scales have the same effect in the three regions. Mann–Kendall test results show that there is an upward trend in the summer periods and a downward trend in the autumn-winter-spring intervals ranging from 10.5 mm/10 years to −37.4 mm/10 years, which affect the local water resources management, droughts mitigation, and agriculture decision making. This situation poses challenges for future study.

Keywords Trend of precipitation · Frequency of drought · Standardized Precipitation Index (SPI) · Mann–Kendall · Gansu Province

1 Introduction

Under current global climate changes, it is necessary to analyze the characteristics of precipitation and drought for the local water resources management, drought hazard mitigation, and to understand the course and patterns of ecological and environmental

L. Zhai · Q. Feng
College of Earth and Environmental Science, Lanzhou University, Lanzhou, China
e-mail: zhailuxin6931@163.com; zhailx05@lzu.cn

Q. Feng (✉)
Cold and Arid Regions Environment and Engineering Research Institute, CAS, Lanzhou, China
e-mail: qifeng@lzb.ac.cn

anomalies (e.g., sandstorms, degeneration of vegetation) in the arid and semi-arid regions. At the same time, changes in precipitation trigger new characteristics of drought in affected regions, especially on spatial distribution and temporal patterns. There is also the necessity of improving the ability of local decision makers to prepare for, and deal with the consequences of precipitation anomalies through the acquisition of a more complete understanding of the range and likelihood of changes in precipitation and drought that a given location has possibly undergone and may experience again (Husak et al. 2007).

The definition and identification of droughts has been an objective of many research efforts for a long time (Łabędzki 2007). Droughts have been sorted into four types (Wilhite and Glantz 1985): meteorological, agricultural, hydrological, and social-economic. In a practical way, there is no universally accepted definition of droughts (Tate and Gustard 2000). Recent studies and investigations show that drought should be defined as a natural but temporary imbalance in water availability, consisting of a persistent lower-than-average precipitation, resulting in diminished water resources availability (Paulo and Pereira 2006; Pereira et al. 2002). Most definitions attribute drought to a breakdown in the rainfall regime. Meteorological drought lasting sufficiently to cause hydrological and agricultural hazards is expressed in terms of rainfall in relation to an average amount and duration of a dry period and can be defined as a period with a lack of precipitation or with rainfall lower than average. Several indices in the monitoring and assessment of drought are used: Standardized Precipitation Index (SPI), Palmer Drought Severity Index (PDSI), Palmer Modified Drought Index (PMDI), Palmer Hydrologic Drought Index (PHDI), and *Z*-Index (Kangas and Brown 2007). On the other hand, some drought indices are based on field conditions: Crop Moisture Index (CMI), Surface Water Supply Index (SWSI), Reclamation Drought Index (RDI), Deciles and Percent of Normal (Ntale and Thian 2003). Among these indices, it has been concluded that the spectral characteristics of the PDSI vary with locations across the USA and that the PDSI has a complex structure with an exceptionally long memory, whereas the SPI is spatially consistent and has a simple structure (Guttman 1998).

McKee et al. (1993) have defined the SPI as the number of standard deviations that the observed cumulative rainfalls at a given time scale would deviate from the long-term mean. As a single numeric value, the SPI can be compared across regions with markedly different climates. The Colorado Climate Center, the Western Regional Climate Center and the National Drought Mitigation Center use the SPI to monitor drought in the USA (Edwards and McKee 1997). The SPI is also recommended for use in an emerging regional drought monitoring system, such as Tehran in Iran (Morid et al. 2006), where the precipitation is similar to that in Gansu Province, Northwest China.

Since cumulative precipitation may not be normally distributed, McKee et al. (1993) transformed the data approximately to the normal domain to standardize the drought index. The flexibility of the time scale of SPI is one of its attractive features because it is possible to experience wet conditions at one time scale and dry conditions at another simultaneously. For example, soil moisture, which typically responds to precipitation relatively quickly, may soon be depleted in a brief drought spell, whereas stream flow and groundwater, which are affected by longer-term precipitation anomalies, may still be relatively normal.

In theory, the time scale of SPI is flexible; however, in practice a monthly precipitation series is ‘smoothed’ with a moving window of width equal to the number of months desired, e.g., a 3-month SPI would use a moving window of a 3-month width. Edwards and McKee (1997) selected a 3-month SPI for a short-term drought index, a 12-month SPI for an intermediate-term drought index, and a 48-month SPI for a long-term drought index.

The window is non-centered such that the filtered series depends only on the present and past values of the time series. The filtered data are broken into 12 monthly time series, which McKee et al. (1993) individually fitted with a gamma distribution that can describe skewed hydrologic variables without needing a log transformation (Chow et al. 1988). It is possible to use other distributions, as long as they fit the data adequately.

Precipitation anomalies and droughts always affect a large number of people and cause tremendous economic losses, environmental damage, and social hardships in Gansu Province, which is situated in a transitory climate zone in Northwest China. Some results of research (Shi et al. 2003) have shown that the climate has changed from warm-dry to warm-wet in Northwest China since 1987. This finding brings to the fore a critical problem: how does the change take place and over what extent? How does it affect the local people and social economy? Other researchers (Li et al. 2004) have indicated that sandstorm days are related to the trend of local precipitation and winter-spring drought severity.

The study area in this paper is Gansu Province, which is located at the northeast of the Qinghai-Tibet Plateau. Because of its geographical position, drought is the dominant hazard and precipitation is an important moisture input in the area. In the summer months, the southwest warm-wet airstreams, impeded by the Qinghai-Tibet Plateau, have difficulty arriving at the Hexi Corridor. Moreover, as influenced by the west Pacific Ocean subtropical high pressure and its position, the warm-humid airstreams coming from Southeast Asia has an annual and seasonal change, which consequently affects the precipitation in Gansu Province. Three climatic regions typify Gansu Province (see Fig. 1): (i) the humid Yangtze River Basin region, located at the north-facing slope of West Qingling Mountain

Fig. 1 Geographical location of the selected pluviometric stations

in the province's southeast, receiving over 400 mm/year in precipitation, (ii) the semi-arid Yellow River Basin region, covering the province's central and eastern portions, receiving 185–780 mm/year in precipitation, and (iii) the arid Inland River Basin region, a long, narrow strip (i.e., the Hexi Corridor, including the basin of Shiyanghe River in the eastern part of the Hexi Corridor, the upstream and middle reaches of Heihe River, and the entire basin of the Shulehe River) located at the western portion of the province, receiving 39.7–34.6 mm/year in precipitation.

Precipitation in Gansu Province fluctuates severely in the inter-annual and decadal time scales. Drought hazards break out frequently in Gansu Province and produce huge losses in agriculture and the social economy. According to drought statistics documents, Gansu suffered 20 drought events in 41 years, from 1949 to 1990. There were 10 extreme droughts during the span of these events (Yin et al. 2005).

In the spring-summer drought of 1953, the farmland area up to 0.89 million hectares of the farmland area in Gansu Province suffered from drought. About 2.52 million people's lives were affected, and the output of grain was reduced by 0.44 million tons. In 1962, the affected land area amounted to 1.14 million hectares. In the same year, the affected population was 3.9 million, and the reduction of grain output amounted to 0.57 million tons. In three consecutive years of drought from 1971 to 1973, the area that suffered from drought was placed at 3.32 million hectares. The disaster population was 17.62 million. The reduction of grain output was 2.15 million tons. The area of disaster mainly covered the Yellow River Basin and the Yangtze River Basin. During the two-year drought from 1981 to 1982, 32 agricultural counties suffered from severe drought. The land that suffered from drought was placed at 1.4 million hectares. The disaster population was 5.2 million and the reduction of grain output was measured at 1.24 million tons. In 1982, 74 counties suffered from severe drought, with the area of the entire province suffering from drought amounting to 1.26 million hectares. The disaster population was placed at 5.52 million. The reduction of grain output rose to 1.31 million tons. In the autumn drought of 1987, the area that suffered from drought was 1.15 million hectares. The disaster population was 5.17 million and the reduction of grain output was placed at 1.1 million tons.

In order to comprehensively understand the trend of the precipitation and characteristics of drought, many researchers have undertaken studies on the dry/wet trend and the frequency of drought in the north of China (Ma and Fu 2006; Ma and Dan 2005; Zhang 1998; Li et al. 2002; Wang and Zhai 2003; Zhang et al. 2003; Zhang and Chen 1991). However, the research on the trend of precipitation at multiple time scales and the characteristic of drought at higher resolution in Gansu Province has not been reported. The objective of this paper is to identify the drought with SPI at different time scales and with higher resolution, detect the trend of precipitation, and analyze the distribution of trend of precipitation and the frequency of drought in Gansu Province. This type of research has not been undertaken in this particular province. The results of this paper could be utilized as a reference for decision making regarding local water resources management, ecological recovery, and drought hazards mitigation.

2 Data and methods

The pluviometric data analyzed in this paper were collected from the China Meteorological Data Sharing Service System (http://cdc.cma.gov.cn/) and the Hydrology and Water Resources Survey Administration of the Gansu Province. A continuous time series from 35 pluviometric stations (see Fig. 1) distributed over the whole region was analyzed with the length of 33–73 years (Table 1). Another 35-station precipitation data series was used as reference when spatial interpolation was conducted. Previous research applying estimated distribution parameters suggests that over 30 years of data were utilized in the estimation of parameters of the SPI (McKee et al. 1993; Hayes et al. 1999; Wu et al. 2001). The Mann–Kendall non-parametric test was used to analyze trend of precipitation and the SPI was used to calculate aridity in the region.

Table 1 Pluviometric stations, periods on record, and locations in the different climatic regions of Gansu Province, Northwest China

Stations		Period (years)	Mean value (mm)	Std. deviation	Climate region
1	Mazongshan	1958–2005 (48)	74.4	29.0	Inland River Basin
2	Donghuang	1938–2005 (68)	39.7	21.0	Inland River Basin
3	Anxi	1951–2005 (55)	48.2	20.0	Inland River Basin
4	Yumenzhen	1953–2005 (53)	62.8	21.5	Inland River Basin
5	Dingxin	1955–2005 (51)	52.6	19.8	Inland River Basin
6	Jingta	1952–2005 (54)	59.0	21.1	Inland River Basin
7	Jiuquan	1935–2005 (71)	84.4	30.2	Inland River Basin
8	Gaotai	1952–2005 (54)	106.0	30.5	Inland River Basin
9	Zhangye	1951–2005 (55)	128.2	32.9	Inland River Basin
10	Shandan	1953–2005 (53)	197.7	44.4	Inland River Basin
11	Yongchang	1954–2005 (52)	201.3	46.1	Inland River Basin
12	Wuwei	1951–2005 (55)	167.0	40.6	Inland River Basin
13	Mingqin	1953–2005 (53)	112.7	34.0	Inland River Basin
14	Wusaoling	1951–2005 (55)	410.5	81.2	Yellow River Basin
15	Sunshan	1956–1988 (33)	265.1	62.7	Yellow River Basin
16	Jingtai	1956–2005 (50)	184.9	51.0	Yellow River Basin
17	Lanzhou	1936–2003 (68)	318.8	71.8	Yellow River Basin
18	Jingyuan	1937–2005 (69)	237.7	61.1	Yellow River Basin
19	Yuzhong	1953–2005 (53)	388.4	81.5	Yellow River Basin
20	Lingxia	1943–2005 (63)	501.6	87.8	Yellow River Basin
21	Lingtao	1933–2005 (73)	504.2	111.1	Yellow River Basin
22	Huining	1956–2000 (45)	410.9	97.8	Yellow River Basin
23	Huajialing	1950–2005 (56)	485.6	108.3	Yellow River Basin
24	Huanxian	1957–2005 (49)	434.6	121.4	Yellow River Basin
25	Pingliang	1942–2005 (64)	506.6	111.8	Yellow River Basin
26	Xifengzhen	1938–2005 (68)	544.9	117.4	Yellow River Basin
27	Maqu	1967–2005 (39)	601.8	89.0	Yellow River Basin
28	Langmusi	1957–1988 (32)	779.9	60.2	Yellow River Basin
29	Hezuo	1958–2005 (48)	543.8	90.4	Yellow River Basin
30	Mingxian	1937–2005 (69)	579.3	86.3	Yellow River Basin
31	Tianshui	1936–2003 (68)	525.0	118.5	Yellow River Basin
32	Zhenning	1956–2000 (45)	616.7	110.4	Yellow River Basin
33	Wudu	1951–2005 (55)	465.0	78.1	Yangtze River Basin
34	Chengxian	1956–2001 (46)	679.3	158.7	Yangtze River Basin
35	Wenxian	1959–2002 (44)	448.7	66.7	Yangtze River Basin

2.1 The Mann–Kendall non-parametric test

The popular non-parametric rank-based Mann–Kendall test (Sneyers 1990) is particularly useful in detecting trends in paired data, as: (i) data need not conform to any particular distribution, thus extreme values are acceptable (Hirsch et al. 1993), (ii) missing values are allowed (Yu et al. 1993), (iii) the use of relative magnitudes (ranking) rather than numerical values allows 'trace' or 'below detection limit' data to be used—they are assigned a lesser value than the smallest measured value, and (iv) in time series analysis, it is unnecessary to specify whether the trend is linear or not (Sneyers 1990; Yu et al. 1993; Silva 2005). The correlation between two variables is termed as the Kendall's correlation coefficient, or Kendall statistic S.

Consider a time series $\{X_i | i = 1, 2, \ldots N\}$ with the record length N. According to Salas (1993) and Yu et al. (1993), the null hypothesis H_0 states that the deseasonalized data $\{X_i\}$ are a sample of n independent and identically distributed random variables. The alternative hypothesis (H_1) of a two-sided test is that the distribution of X_i and X_j are not identical for all $i, j \leq N$ with $i \neq j$. Each value X_i, $i = 1, \ldots N - 1$ is compared with all subsequent values $\{X_j | j = i + 1, i + 2, \ldots N\}$ and sum the times of $X_j > X_i$. The number of positive difference for all the differences considered, p, is given by

$$p = \sum_i n_i \tag{1}$$

The Mann–Kendall statistic, S, is calculated as

$$S = (4p/(N(N-1))) - 1, \tag{2}$$

where p is the number of positive differences for all the differences considered.

Under the H_0 hypothesis, the distribution of S is normal in the limit as $N \to \infty$ (Yu et al. 1993). The mean and variance of S are calculated as:

$$E(S) = 0, \tag{3}$$

$$\mathrm{Var}(S) = 2(2N+5)/(9N(N-1)), \tag{4}$$

For $N > 10$, the test is conducted using a normal approximation (Hirsch et al. 1993). The standardized test statistic, M, is calculated as:

$$M = S/(\mathrm{Var}(S))^{1/2} \tag{5}$$

Hisdal et al. (2001) accentuated that the hypothesis (H_1) of an upward or downward trend cannot be rejected at significance level α if $|M| > M_{(1-\alpha/2)}$, where $M_{(1-\alpha/2)}$ is the $1 - \alpha/2$ quantile of the standard normal distribution. When a positive value of M indicates an upward trend, a negative value of M indicates a downward trend. $|M| > 1.96$ indicates a significant upward/downward trend (at a significance level of $\alpha = 0.05$) and $|M| > 2.576$ indicates an extremely significant trend (at a significance level of $\alpha = 0.01$). In this paper, after deriving the Mann–Kendall test statistic, M, of every monthly data series, spatial interpolate was used to interpolate M and realize the trend distribution over the province.

2.2 Standardized Precipitation Index

The SPI is widely accepted and used throughout the world in both research and operational management since it is normalized to a location and normalized in time (Wu et al. 2007).

Practically, when one computes the SPI, it is enough to do so with pluviometric data, and there is no need to investigate the soil moisture, temperature, among others, in contrast to the process of calculating the Palmer Drought Severity Index (PDSI).

To derive the SPI, a gamma probability density function to a given frequency distribution of precipitation totals for the station of interest is fitted as (Edwards and McKee 1997)

$$g(x) = \frac{1}{\beta^{\alpha}\Gamma(\alpha)} x^{\alpha-1} \mathrm{e}^{-x/\beta} \quad \text{for } x > 0 \tag{6}$$

where α is a shape parameter ($\alpha > 0$), β, is a scale parameter ($\beta > 0$), x is the precipitation amount ($x > 0$), and

$$\Gamma(\alpha) = \int\limits_0^{\infty} y^{\alpha-1} \mathrm{e}^{-y} \mathrm{d}y$$

where $\Gamma(\alpha)$ is the gamma function.

The shape parameter α and the scale parameter β are estimated for each time scale of interest (either weeks or months) and for each week or month of the year, depending on whether the weekly or monthly SPI is calculated:

$$\hat{\alpha} = \frac{1}{4A}\left(1 + \sqrt{1 + \frac{4A}{3}}\right) \tag{7}$$

$$\hat{\beta} = \frac{\bar{x}}{\hat{\alpha}} \tag{8}$$

where

$$A = \ln(\bar{x}) - \frac{1}{n}\sum_{i=1}^{n} \ln(x_i)$$

n is the number of precipitation observations and $\bar{x}$ is the mean precipitation over the time scale of interest, x_i is the sample of the pluviometric data, and A is a measure of the skewness of distribution (Husak et al. 2007). For the calculation of $\bar{x}$ and $\ln x_i$, it must be noted that only the number of weeks or months with positive accumulations were used, and only the non-zero observations in the records were utilized in the estimation of the gamma distribution parameters (Husak et al. 2007).

The cumulative probability of each observed precipitation event for a given time scale for the station of interest is computed by the estimated shape and scale parameters. An equal-probability transformation is made from the cumulative probability to the standard normal random variable Z with the value of the mean as zero and of the variance as one, where the SPI takes on the value of Z.

The cumulative probability is given by

$$G(x) = \int\limits_0^{x} g(x)\mathrm{d}x = \frac{1}{\hat{\beta}^{\hat{\alpha}}\Gamma(\hat{\alpha})} \int\limits_0^{x} x^{\hat{\alpha}-1} \mathrm{e}^{-x/\hat{\beta}} \mathrm{d}x \tag{9}$$

Letting $t = x/\hat{\beta}$, this equation becomes the incomplete gamma function

$$G(x) = \frac{1}{\Gamma(\hat{\alpha})} \int_0^x t^{\hat{\alpha}-1} e^{-t} dt \tag{10}$$

Since the gamma function is undefined for $x = 0$ and a precipitation distribution may contain zeros, the cumulative probability becomes

$$H(x) = q + (1 - q)G(x) \tag{11}$$

where q is the probability of a zero. If m is the number of zeros in a precipitation time series, q can be estimated by m/n (Thom 1966).

The cumulative probability, $H(x)$, is then transformed into the standard normal random variable Z ($\mu = 0$, $\sigma^2 = 1$), which is the value of the SPI.

Since it would be cumbersome to produce these types of figures for all stations at all time scales and for each month of the year, the Z or SPI value is more easily obtained computationally using an approximation provided by Abramowitz and Stegun (1965) that converts cumulative probability to the standard normal random variable Z:

$$Z = \mathrm{SPI} = -\left(t - \frac{c_0 + c_1 t + c_2 t^2}{1 + d_1 t + d_2 t^2 + d_3 t^3}\right) \quad 0 < H(x) \le 0.5 \tag{12}$$

$$Z = \mathrm{SPI} = \left(t - \frac{c_0 + c_1 t + c_2 t^2}{1 + d_1 t + d_2 t^2 + d_3 t^3}\right) \quad 0.5 < H(x) < 1.0 \tag{13}$$

where

$$t = \sqrt{\ln\left(\frac{1}{(\ln H(x))^2}\right)} \quad 0 < H(x) \le 0.5$$

$$t = \sqrt{\ln\left(\frac{1}{(1 - \ln H(x))^2}\right)} \quad 0.5 < H(x) < 1.0$$

$c_0 = 2.515517$, $c_1 = 0.802853$, $c_2 = 0.010328$, $d_1 = 1.432788$, $d_2 = 0.189269$, $d_3 = 0.001308$.

The calculations of the SPI and the Mann–Kendall test statistic M in this paper were performed by MATLAB software.

3 Results

3.1 Spatial and temporal distribution of trend of the precipitation

For every station's monthly and annual precipitation time series, the rate of change in precipitation with time (slope) was calculated by least-squares linear fitting, and Mann–Kendall test results were determined (Table 2). With the exception of the Lintao, Mingxian, and Chengxian stations, all stations within the Yellow River Basin and Yangtze River Basin showed no significant trend in annual precipitation. The slope of the annual series of the Mingxian and Chengxian stations showed decadal changes in precipitation to be generally negative, ranging from −10.0 mm/10 years to −37.4 mm/10 years. However, the slope of annual precipitation of the Lintao station was 10.0 mm/10 years. Slightly

Table 2 Results of the application of the Mann–Kendall test and of least-squares linear fitting to the mean yearly and monthly precipitation for all pluviometric data series[a]

Stations	Year (mm decade^{-1})		January (mm decade^{-1})		February (mm decade^{-1})		March (mm decade^{-1})		April (mm decade^{-1})		May (mm decade^{-1})		June (mm decade^{-1})	
	M	$b \pm \sigma$	*M*	$b \pm \sigma$	*M*	$b \pm \sigma$	*M*	$b \pm \sigma$	*M*	$b \pm \sigma$	*M*	$b \pm \sigma$	*M*	$b \pm \sigma$
Mazongshan	−1.51	−4.5 ± 28	−1.97*	−0.3 ± 1	−2.77**	−0.2 ± 1	−0.91	0.2 ± 3	−1.48	−0.2 ± 4	−1.35	−0.4 ± 8	−0.05	0.4 ± 11
Donghuang	0.62	0.2 ± 21	−1.48	0.0 ± 1	−3.41**	−0.2 ± 2	−1.22	0.0 ± 4	−0.89	0.0 ± 4	−0.3	0.2 ± 6	0.42	0.1 ± 10
Anxi	1.74	1.9 ± 20	−1.63	−0.1 ± 2	−3.84**	−0.6 ± 3	0.18	0.5 ± 4	−0.98	0.0 ± 4	0.21	−0.3 ± 6	0.65	0.5 ± 9
Yumenzhen	0.89	2.0 ± 21	−1.14	0.0 ± 2	−2.96**	−0.6 ± 3	0.46	0.5 ± 5	−0.38	−0.3 ± 5	1.38	0.1 ± 11	0.91	1.0 ± 10
Dingxin	0.04	0.1 ± 20	−3.5**	−0.1 ± 1	−2.87**	0.0 ± 1	−0.87	0.5 ± 3	−2.93**	−0.6 ± 3	−1.11	−0.5 ± 6	0.35	0.6 ± 7
Jingta	1.71	2.0 ± 21	−0.46	0.0 ± 1	−2.68**	−0.4 ± 2	0.89	0.9 ± 5	−1.23	−0.2 ± 3	0.08	−0.6 ± 9	0.63	0.4 ± 7
Jiuquan	−0.22	−0.5 ± 30	−0.26	0.1 ± 2	−2.54*	−0.4 ± 3	1.32	0.5 ± 7	−1.19	−0.4 ± 5	0.93	0.1 ± 13	0.93	0.7 ± 11
Gaotai	0.99	2.0 ± 30	−0.46	0.1 ± 2	−1.6	0.0 ± 1	0.32	0.5 ± 6	−0.13	0.1 ± 5	0.77	−0.1 ± 13	0.16	0.5 ± 11
Zhangye	−0.25	−0.9 ± 33	−0.31	0.0 ± 2	−1.37	0.0 ± 1	0.21	0.2 ± 5	−0.54	−0.1 ± 5	−0.01	0.0 ± 12	0.34	0.6 ± 13
Shandan	0.4	3.6 ± 44	−0.15	0.0 ± 2	−1.01	0.0 ± 2	0.52	0.4 ± 6	−0.37	−0.1 ± 6	1.1	0.6 ± 13	0.83	2.2 ± 19
Yongchang	1.83	5.0 ± 46	0.21	0.2 ± 1	0.09	0.1 ± 2	1.22	0.6 ± 5	0	−0.3 ± 6	0.76	0.9 ± 15	1.59	3.7 ± 22
Wuwei	1.22	6.3 ± 39	−1.21	0.0 ± 2	−1.61	−0.1 ± 2	1.22	1.0 ± 6	0.45	0.0 ± 5	2.35*	1.4 ± 11	2.93**	3.5 ± 18
Mingqin	0.18	1.3 ± 34	−3.53**	−0.1 ± 1	−0.66	0.2 ± 1	−1.83	−0.1 ± 4	0.09	0.1 ± 5	1.33	1.3 ± 10	0.75	1.7 ± 15
Wusaoling	−0.91	−6.2 ± 81	0.72	0.0 ± 2	0.21	−0.3 ± 3	0.15	−0.2 ± 9	−2.94**	−2.4 ± 10	0.04	0.1 ± 22	0.38	0.8 ± 24
Sunshan	0.62	7.2 ± 62	−1.27	−0.4 ± 1	−0.06	0.0 ± 2	0.12	0.1 ± 4	−0.5	−0.6 ± 8	1.02	1.9 ± 15	1.18	4.9 ± 16
Jingtai	0.38	1.0 ± 51	−1.85	0.0 ± 1	−0.26	0.1 ± 2	0.66	0.4 ± 5	−1.31	−1.0 ± 8	−0.23	0.1 ± 14	1.36	2.8 ± 18
Lanzhou	−0.06	−1.7 ± 72	−0.73	0.0 ± 2	−0.7	0.0 ± 2	0.43	0.1 ± 6	0.39	0.4 ± 12	0.28	1.4 ± 26	1.75	2.0 ± 24
Jingyuan	−0.61	−2.1 ± 61	−0.54	0.0 ± 3	−1.44	−0.3 ± 3	−0.77	−0.2 ± 5	−0.23	0.0 ± 11	1.58	2.1 ± 18	0.83	0.7 ± 19
Yuzhong	−0.66	−8.2 ± 81	−0.69	−0.2 ± 2	0.87	0.2 ± 3	0.64	0.3 ± 8	0.17	−0.4 ± 18	0.57	2.3 ± 29	0.98	3.4 ± 27
Lingxia	−0.61	−2.9 ± 88	−0.75	−0.1 ± 3	0.66	0.2 ± 4	1.25	0.6 ± 11	0.12	0.1 ± 19	0.21	1.2 ± 34	−0.02	0.8 ± 29
Lingtao	1.96*	10.5 ± 109	0.98	0.1 ± 3	0.46	0.1 ± 4	1.21	0.6 ± 9	2.27*	2.3 ± 20	1.39	2.7 ± 33	1.8	2.6 ± 28
Huining	−1.68	−20.7 ± 94	0.47	0.2 ± 3	0.33	0.2 ± 5	−0.14	−0.4 ± 8	0.33	0.7 ± 16	−0.47	−2.9 ± 26	0	0.3 ± 27
Huajialing	−0.98	−9.1 ± 107	0.82	0.0 ± 4	−1.09	−0.7 ± 5	−0.58	−0.5 ± 7	−0.58	−0.7 ± 18	0.81	1.1 ± 29	0.2	0.9 ± 29
Huanxian	−0.95	−12.3 ± 120	−0.57	0.1 ± 2	−0.53	−0.1 ± 4	−0.34	0.2 ± 10	−0.36	0.0 ± 17	−0.36	0.6 ± 28	2.47*	8.3 ± 30

Table 2 continued

Stations	Year (mm decade^{-1})		January (mm decade^{-1})		February (mm decade^{-1})		March (mm decade^{-1})		April (mm decade^{-1})		May (mm decade^{-1})		June (mm decade^{-1})	
	M	$b \pm \sigma$	*M*	$b \pm \sigma$	*M*	$b \pm \sigma$	*M*	$b \pm \sigma$	*M*	$b \pm \sigma$	*M*	$b \pm \sigma$	*M*	$b \pm \sigma$
Pingliang	−0.78	−5.9 ± 111	0	−0.1 ± 3	0.82	0.0 ± 4	0.13	−0.1 ± 10	−1.84	−1.6 ± 17	−1.18	−1.9 ± 31	0.42	2.5 ± 38
Xifengzhen	−0.1	−0.2 ± 117	0.46	−0.1 ± 5	−0.11	−0.4 ± 7	0.83	0.5 ± 12	0.1	0.3 ± 22	−0.49	−0.9 ± 34	1.05	0.6 ± 40
Maqu	−0.5	−9.9 ± 88	−0.28	0.0 ± 3	0.28	0.4 ± 4	−0.23	−0.2 ± 6	−0.54	−0.9 ± 12	0.04	0.1 ± 23	0.28	1.5 ± 28
Langmusi	0.03	2.8 ± 121	−1.59	−1.5 ± 4	−0.06	0.3 ± 6	0.42	−0.1 ± 11	−0.36	0.2 ± 18	0.19	0.0 ± 34	1.43	11.6 ± 39
Hezuo	−1.14	−11.7 ± 89	1.35	0.5 ± 3	2.42*	0.9 ± 3	1.42	1.8 ± 9	0.04	0.2 ± 16	−0.46	−3.5 ± 30	1.37	3.7 ± 29
Mingxian	−2.03*	−10.0 ± 84	0.1	0.0 ± 2	−1.6	−0.3 ± 4	0.01	0.2 ± 9	−0.19	−0.7 ± 20	−0.95	−1.6 ± 30	1.67	2.5 ± 26
Tianshui	−1.87	−11.0 ± 116	2.26*	0.5 ± 3	−0.35	0.0 ± 5	1.11	0.5 ± 9	0.02	0.2 ± 20	−1.31	−2.3 ± 27	−0.25	−1.8 ± 38
Zhenning	−0.51	−9.4 ± 110	−0.37	−0.1 ± 4	−1.58	−1.0 ± 6	−1.08	−1.1 ± 10	−1.7	−2.4 ± 23	−0.9	−2.6 ± 34	1.8	2.7 ± 36
Wudu	−1.68	−9.6 ± 77	−0.01	0.1 ± 3	−0.25	−0.1 ± 3	−0.08	−0.1 ± 7	−1.01	−1.5 ± 16	0.09	0.8 ± 24	0.62	1.4 ± 32
Chengxian	−2.09*	−37.4 ± 151	0.84	0.5 ± 5	0.29	0.3 ± 5	−0.39	−0.4 ± 11	−0.84	−2.0 ± 25	−0.29	−2.0 ± 34	0.16	−5.9 ± 59
Wenxian	−1.27	−5.6 ± 66	−1.46	−0.4 ± 2	0.18	0.1 ± 2	0.34	0.4 ± 6	1.27	2.0 ± 14	1.34	4.4 ± 27	0.38	0.1 ± 30

Stations	Year (mm decade^{-1})		July (mm decade^{-1})		August (mm decade^{-1})		September (mm decade^{-1})		October (mm decade^{-1})		November (mm decade^{-1})		December (mm decade^{-1})	
	M	$b \pm \sigma$	*M*	$b \pm \sigma$	*M*	$b \pm \sigma$	*M*	$b \pm \sigma$	*M*	$b \pm \sigma$	*M*	$b \pm \sigma$	*M*	$b \pm \sigma$
Mazongshan	−1.51	−4.5 ± 28	−2.72**	−3.8 ± 18	−0.84	−0.4 ± 11	−0.41	−0.5 ± 7	−0.75	0.4 ± 3	0.28	0.3 ± 2	−2.35*	−0.1 ± 1
Donghuang	0.62	0.2 ± 21	0.55	−0.1 ± 12	0.3	0.1 ± 6	−2.34*	0.0 ± 3	−5.75**	0.1 ± 1	−2.67**	0.0 ± 2	−2.13*	0.0 ± 2
Anxi	1.74	1.9 ± 20	0.08	−0.1 ± 12	1.23	1.0 ± 9	−0.69	0.4 ± 4	−1.97*	0.3 ± 3	−2.49*	0.1 ± 2	0.4	0.2 ± 1
Yumenzhen	0.89	2.0 ± 21	−1.15	−0.8 ± 12	0.84	0.9 ± 10	0.38	0.6 ± 6	−1.7	0.1 ± 3	0.03	0.1 ± 3	1.12	0.4 ± 2
Dingxin	0.04	0.1 ± 20	0.17	0.1 ± 12	−0.53	−0.2 ± 9	−0.14	0.1 ± 7	−3.87**	0.0 ± 2	−2.04*	0.0 ± 2	−2.07*	0.1±1
Jingta	1.71	2.0 ± 21	0.89	0.8 ± 13	0.5	0.6 ± 11	−0.28	0.2 ± 7	−1.02	0.3 ± 3	−1.05	0.3 ± 2	−1.92	−0.3 ± 2
Jiuquan	−0.22	−0.5 ± 30	−0.61	−0.2 ± 16	−1.1	−1.6 ± 16	0.7	0.4 ± 10	−0.47	0.3 ± 3	−1.22	−0.1 ± 3	−1.42	−0.1 ± 2
Gaotai	0.99	2.0 ± 30	0.43	0.8 ± 18	−0.6	−1.1 ± 14	0.4	0.3 ± 12	−0.07	0.6 ± 5	−0.5	0.2 ± 3	0.59	0.1 ± 2
Zhangye	−0.25	−0.9 ± 33	0.5	0.4 ± 17	−1.27	−1.9 ± 17	0.17	0.2 ± 14	−0.43	−0.1 ± 5	−1.68	−0.1 ± 3	0.21	0.0 ± 2

Table 2 continued

Stations	Year (mm decade^{-1})		January (mm decade^{-1})		February (mm decade^{-1})		March (mm decade^{-1})		April (mm decade^{-1})		May (mm decade^{-1})		June (mm decade^{-1})	
	M	$b \pm \sigma$	*M*	$b \pm \sigma$	*M*	$b \pm \sigma$	*M*	$b \pm \sigma$	*M*	$b \pm \sigma$	*M*	$b \pm \sigma$	*M*	$b \pm \sigma$
Shandan	0.4	3.6 ± 44	1.35	2.5 ± 22	−2.03*	−3.5 ± 22	0.64	1.5 ± 21	0.02	0.0 ± 8	−0.08	0.0 ± 4	1.56	0.1 ± 2
Yongchang	1.83	5.0 ± 46	1.77	3.8 ± 20	−1.06	−3.0 ± 27	0.14	0.1 ± 22	−0.6	−1.3 ± 11	0.11	0.1 ± 4	1.09	0.1 ± 1
Wuwei	1.22	6.3 ± 39	1.79	1.2 ± 15	−1.27	−0.7 ± 25	−1.2	0.5 ± 17	0.82	−0.3 ± 9	−1.1	−0.2 ± 5	−0.68	0.0 ± 2
Mingqin	0.18	1.3 ± 34	1.63	2.2 ± 16	−2.29*	−4.6 ± 19	0.35	0.8 ± 12	0.48	−0.1 ± 7	−1.98*	−0.2 ± 4	−2.79**	0.0 ± 1
Wusaoling	−0.91	−6.2 ± 81	0.18	−0.1 ± 32	−0.49	−2.8 ± 37	0.31	−0.6 ± 27	0.34	0.3 ± 9	−1.05	−0.6 ± 4	−0.23	−0.2 ± 2
Sunshan	0.62	7.2 ± 62	−0.34	2.3 ± 32	−0.59	−3.7 ± 25	0.46	0.8 ± 19	1.02	2.2 ± 8	−0.96	−0.3 ± 3	−0.22	0.1 ± 1
Jingtai	0.38	1.0 ± 51	0.68	1.8 ± 23	−0.78	−3.2 ± 25	0.79	0.0 ± 21	0.23	0.1 ± 10	−2.15*	−0.2 ± 3	−4.78**	0.0 ± 1
Lanzhou	−0.06	−1.7 ± 72	0.15	1.0 ± 31	−1.07	−3.0 ± 41	−2.35*	−3.7 ± 24	0.82	0.7 ± 16	−2.38*	−0.4 ± 5	−3.07**	−0.1 ± 2
Jingyuan	−0.61	−2.1 ± 61	0.44	0.4 ± 28	−1.14	−2.2 ± 30	−1.84	−2.4 ± 19	1	0.6 ± 12	−2.88*	−0.7 ± 4	−4.35**	−0.1 ± 1
Yuzhong	−0.66	−8.2 ± 81	0.02	0.0 ± 40	−1.27	−6.7 ± 45	−1.63	−4.4 ± 28	−1.04	−1.6 ± 17	−1.49	−0.8 ± 5	−2.53*	−0.4 ± 2
Lingxia	−0.61	−2.9 ± 88	0.97	1.9 ± 38	−0.21	−3.0 ± 46	−2.39*	−4.9 ± 32	0.71	0.5 ± 19	−0.98	−0.3 ± 5	0.3	0.0 ± 2
Lingtao	1.96*	10.5 ± 109	0.29	0.9 ± 43	0.38	1.4 ± 54	−0.61	−1.6 ± 29	1.64	1.7 ± 18	−0.99	−0.3 ± 7	−0.76	0.0 ± 3
Huining	−1.68	−20.7 ± 94	0.06	−4.5 ± 40	−0.7	−3.1 ± 42	−2.13*	−8.1 ± 33	−0.57	−1.6 ± 17	−1.82	−1.6 ± 7	−0.57	0.2 ± 3
Huajialing	−0.98	−9.1 ± 107	0.66	2.1 ± 44	−1.09	−4.8 ± 53	−0.99	−3.6 ± 35	−0.51	−0.8 ± 18	−2.63**	−1.6 ± 6	−1.96*	−0.5 ± 4
Huanxian	−0.95	−12.3 ± 120	−0.14	−2.1 ± 57	−0.47	−5.7 ± 61	−2.19*	−8.5 ± 40	−0.24	−2.2 ± 21	−2.45*	−2.7 ± 10	−1.03	−0.1 ± 4
Pingliang	−0.78	−5.9 ± 111	0.92	3.6 ± 56	−0.34	−3.0 ± 58	−1.37	−5.3 ± 50	1.07	1.2 ± 23	−1.75	−1.0 ± 10	−0.76	−0.2 ± 4
Xifengzhen	−0.1	−0.2 ± 117	0.23	0.9 ± 49	−0.3	0.1 ± 60	−0.43	−0.8 ± 52	1.18	1.2 ± 27	−1.88	−1.5 ± 12	−0.24	0.0 ± 5
Maqu	−0.5	−9.9 ± 88	1.25	6.3 ± 43	−0.79	−4.9 ± 47	−2	−11.8 ± 36	0.16	−0.5 ± 24	−0.16	−0.3 ± 5	1.29	0.3 ± 2
Langmusi	0.03	2.8 ± 121	0.16	0.8 ± 55	−0.88	−3.9 ± 60	0.06	0.7 ± 56	−0.65	−3.7 ± 31	−1.14	−1.5 ± 7	0.71	0.0 ± 3
Hezuo	−1.14	−11.7 ± 89	−0.14	−1.2 ± 40	−1.8	−8.8 ± 42	−1.37	−4.0 ± 29	−0.3	−0.8 ± 17	−0.82	−0.6 ± 4	0.28	0.1 ± 2
Mingxian	−2.03*	−10.0 ± 84	−2.1*	−5.4 ± 38	−0.91	−1.4 ± 40	−2.09*	−3.5 ± 34	0.17	0.2 ± 20	−0.41	−0.1 ± 5	−0.35	0.1 ± 2
Tianshui	−1.87	−11.0 ± 116	−0.15	−1.8 ± 45	−1.4	−4.9 ± 54	−1.65	−3.3 ± 42	1.74	2.3 ± 21	−1.03	−0.7 ± 9	0	0.1 ± 4
Zhenning	−0.51	−9.4 ± 110	0.9	3.6 ± 48	−0.12	1.6 ± 59	−1.23	−8.3 ± 55	0.37	0.8 ± 32	−0.55	−2.5 ± 17	−0.23	0.0 ± 5
Wudu	−1.68	−9.6 ± 77	−1.55	−4.1 ± 36	−0.59	−1.8 ± 40	−0.15	−1.1 ± 31	−1.69	−2.0 ± 15	−1.3	−1.0 ± 7	−2.24*	−0.1 ± 1

Table 2 continued

Stations	Year (mm decade^{-1})		January (mm decade^{-1})		February (mm decade^{-1})		March (mm decade^{-1})		April (mm decade^{-1})		May (mm decade^{-1})		June (mm decade^{-1})	
	M	$b \pm \sigma$	M	$b \pm \sigma$	M	$b \pm \sigma$	M	$b \pm \sigma$	M	$b \pm \sigma$	M	$b \pm \sigma$	M	$b \pm \sigma$
Chengxian	−2.09*	−37.4 ± 151	−0.96	−9.0 ± 66	−1.13	−10.7 ± 68	−0.88	−6.2 ± 55	0.18	0.8 ± 25	−2.36*	−3.1 ± 11	0.26	0.3 ± 4
Wenxian	−1.27	−5.6 ± 66	−1.07	−5.2 ± 33	−0.34	−1.2 ± 30	−1.11	−3.6 ± 29	−0.49	−1.2 ± 15	−1.25	−0.7 ± 6	−2.37*	−0.5 ± 4

[a] b (percentage contribution/decade) is the linear regression coefficient, σ is the root mean square of error, M is the Mann–Kendall test value

* Significance level >95%

** Extremely significance level >99%

positive yet non-significant Mann–Kendall test values and slopes were obtained for all the Inland River Basin stations except the Mazongshan, Jiuquan, and Zhangye stations, where precipitation increased by 0.1–6.3 mm/10 years over the period of analysis. The changes in annual precipitation indicate that on an annual time scale, the Inland River Basin received more water than the Yellow River Basin and Yangtze River Basin.

To assess precipitation trends on a monthly scale, the Mann–Kendall tests and slope fittings were also applied to the monthly precipitation time series from all pluviometric stations investigated (Table 2). From Table 2, it is shown that March marks a climatic transition point in the climate of Gansu Province and of Northwest China as a whole (Wang et al. 1998; Ren et al. 2006), and this month's rainfall is important to the region's natural ecosystems and agricultural production. However, no significant trends in precipitation were found for this month for any station, suggesting that global climate change has yet to impact March precipitation in this region. Comparatively, the Inland River Basin had significant (up to $\alpha = 0.01$, for some stations) changes in precipitation observed in February, October, November, and December for 23.1–53.8% of the stations. Similarly, in the Yellow River Basin, 26.3% of the stations showed significant trends in precipitation for September, November, and December, indicating that precipitation in February, September, November, and December is subject to global atmospheric circulation (Xu et al. 2002).

These changes in precipitation were analyzed for every station based on the slope and standard deviation of least-squares linear fitting (Table 2). For the Inland River Basin, January, February, April, and July through December precipitations showed a negative slope (maximum of −1.3, −3.6, −3.6, −21.8, −25.5, −3.0, −3.3, −4.2, and −2.0 mm/10 years, respectively), whereas a positive slope was apparent in May and June (maximum of 3.6 and 21.5 mm/10 years, respectively). In the Yellow River Basin, March, May, August, and October precipitation showed no significant ($\alpha = 0.05$) trend, whereas the data for September, November, and December precipitation showed a negative slope (maximum of −48.5, −12.7 and −4.5 mm/10 years). In the Yangtze River Basin, only the months of November and December showed a negative slope (maximum of −14.1 and −4.5 mm/10 years), indicating that fall, winter, and spring precipitation, which are important to agriculture production, urban and rural water supplies, and sandstorm prevention, are declining across most of Gansu Province. As a consequence, a more efficient management of water resources is needed to meet the requirements of agriculture and drinking water supplies.

To further confirm the pattern of the spatial and temporal trends, the monthly Mann–Kendall test values were spatially interpolated (see Fig. 2). For January, the results show a downward trend in monthly precipitation for the Inland River Basin, the Yangtze River Basin, and the northwest portion of the Yellow River Basin. Only the southeast of the Yellow River Basin (Dingxi, Tianshui, Pingliang, and Qingyang stations) and the upstream of the Shiyanghe River Basin show an upward trend in precipitation. The significant downward trend was mainly located in the western portion of Gansu Province, near Xingjiang, downstream from the Shiyang River Basin and northeast of Jiuquan. The other regions did not show statistically significant trends for January.

In February, the trend of the precipitation in the west of the Hexi Corridor shifted more critically toward dry conditions. Similarly, a downward trend covered the eastern portion of Gansu Province, including the eastern portions of the Inland River Basin, Yangtze River Basin, and Yellow River Basin. A noticeable yet non-significant negative trend was apparent across the province in November, while a similar positive trend was seen in June. Moreover, the findings reveal that on a climatological basis, the months of July, August, and September are traditionally rainy, whereas December, January, and February are traditionally very dry in Gansu Province. In order to validate the contribution of a month's precipitation trend to the annual total, the correlations between annual trend and monthly trend were analyzed. The correlation coefficients amounted to 0.50, 0.34, 0.53, 0.38, and 0.40 ($P < 0.05$) in May, June, July, August, and September, respectively, and other months' data were obviously less compared to these values. Furthermore, due to the changes in precipitation during some months, the trend of other months were concealed to a great extent, and there was no annual significant trend except for the observations at the three stations (Lintao, Mingxian, and Chengxian). It can be concluded that the changes in monthly precipitation cancel one another out. Consequently, July, August, and September can certainly be considered playing the main role in determining yearly trends. A rainy summer-fall and dry winter-spring would result in flooding conditions in the fall and insufficient soil moisture in the spring, thus adversely affecting the growth of the wheat, which is widely planted in Gansu Province.

The trends in the total annual rainfall (figure not shown) suggest that there was an upward trend in precipitation for the Inland River Basin and the mid-west portion of the

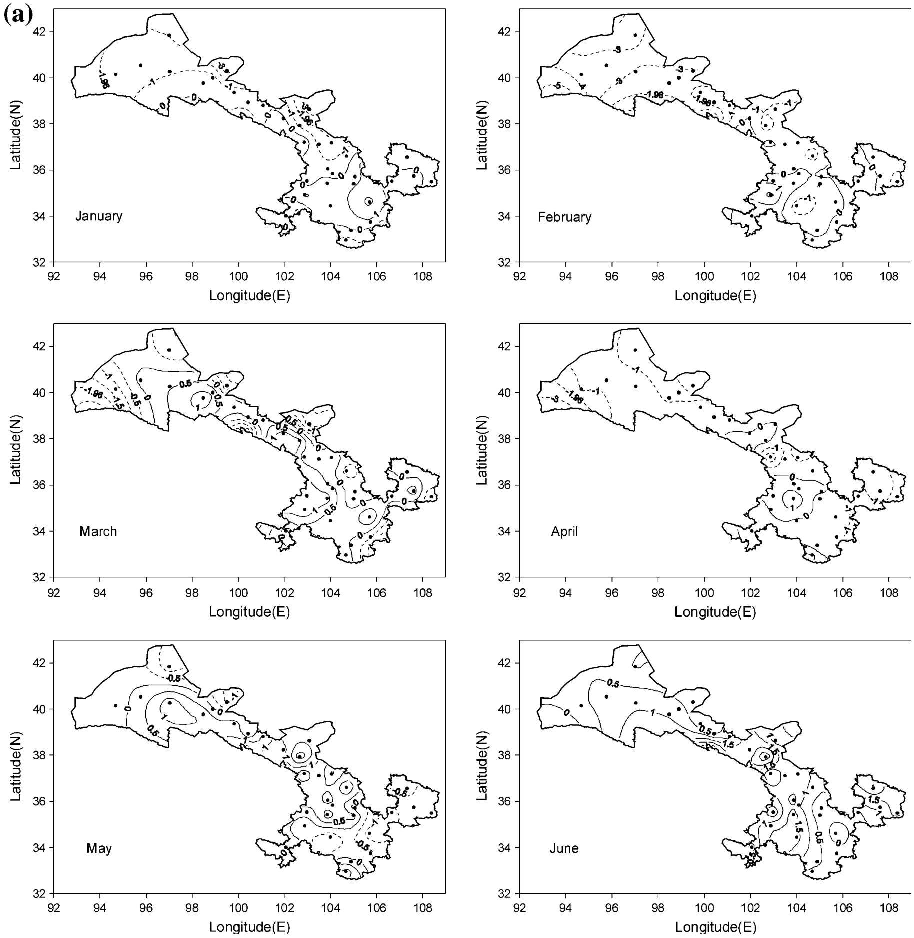

Fig. 2 Results of the MK test for every month. Solid contours represent positive values and dashed negative values

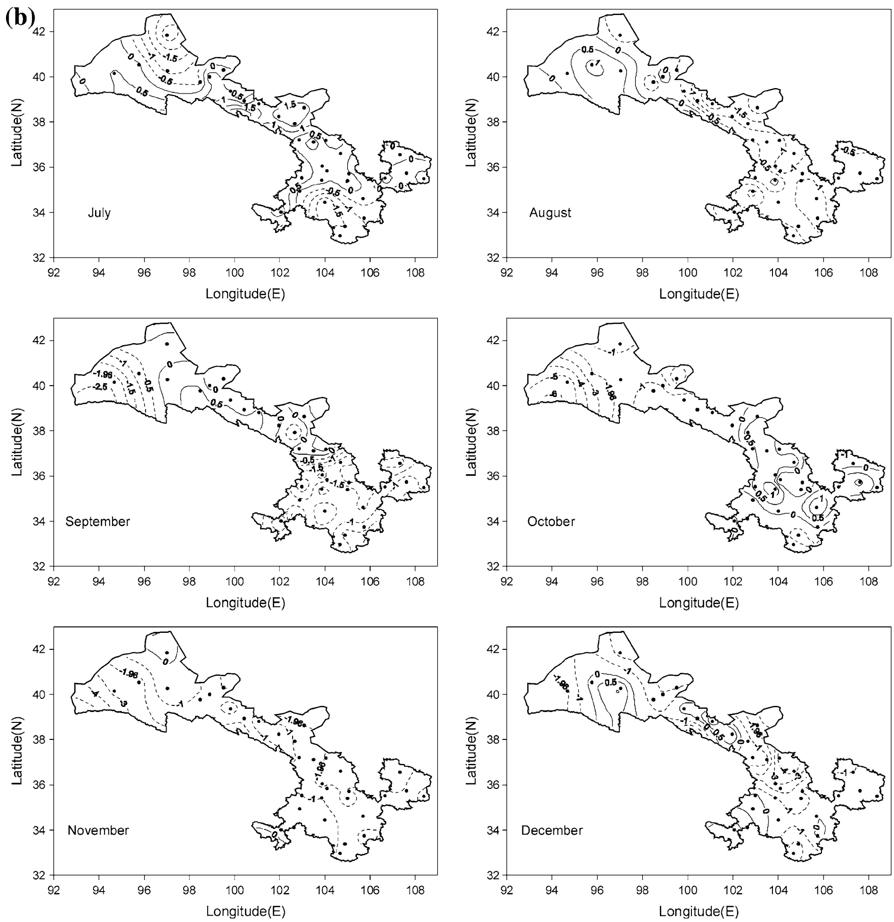

Fig. 2 continued

Yellow River Basin, particularly at the Lintao station. In contrast, a downward trend in precipitation is evident for the southeast portion of the province, including the Dingxi, Longnan, Tianshui, Pingliang, and Qinyang stations. Consequently, more attention should be focused on the threat of droughts in the southeast portion of Gansu Province.

3.2 Spatial and temporal pattern of drought

Drought was identified by the criterion of the SPI. While the value of SPI is theoretically unbound, it is extremely rare empirically to observe values greater than +3.0 or less than −3.0 (Table 3).

With pluviometric data series for over 30 years with no missing data, parameter estimation would be precise (Wu et al. 2005). Hence, stations with such records were selected in the estimation of the parameter of the Gamma function as outlined above.

A representative example of a temporal pattern in SPI is given for the Lanzhou station (see Fig. 3). In order to check whether the SPI can be used to represent drought distribution

Table 3 SPI and corresponding cumulative probability in relation to the base period and nominal class

SPI value	Cumulative probability	Nominal SPI class
−2.0	0.0228	Extremely dry
−1.5	0.0668	severely dry
−1.0	0.1587	Dry
−0.5	0.3085	Normal
0.0	0.5000	Normal
+0.5	0.6915	Normal
+1.0	0.8413	Wet
+1.5	0.9332	Very wet
+2.0	0.9772	Extremely wet

and to analyze drought characteristics at a give time, the SPI of a 6-month (January–June 1962) drought event was derived through a spatial interpolation method (see Fig. 4). According to the statistics of the Office of State Flood Control and Drought Relief Headquarters, there had been less rainfall all over Gansu Province in Northwest China in 1962. Continuous extreme drought went on from spring to summer in some regions such as Tianshui, Pingliang, Qinyang, Dingxi, Lanzhou, Hezuo, Wudu, Jingyuan, Jiuquan, and Zhangye, and caused great economical losses. The results shown in Fig. 4 are consistent with the 1962-measured drought statistics for Gansu Province.

3.3 Frequency of drought

The number of months N_i in each class of drought intensity according to Table 3 was computed for the 3-, 6-, 12-, 24-, and 48-month timescales. Then, the number of droughts per 100 years was calculated as (Łabędzki 2007)

$$N_{i,100} = \frac{N_i}{i \cdot n} \cdot 100 \tag{14}$$

where $N_{i,100}$, the number of droughts for a timescale i in 100 years, N_i, the number of months with drought for a timescale i in the n-year set, i, the timescale (1, 3, 6, 9, 12, 24, 48 months), n, the number of years in the data set (33–77).

The SPIs limitations include its inability to define a drought in areas of extremely low precipitation at small time scales, where a zero or near zero number of droughts occurred for the entire time period using the 1- and occasionally 3-month SPI. This was the result of the median of the precipitation for these areas, for the periods on record, being zero. When the time scales were increased and more months were considered, this problem was solved (Kangas and Brown 2007). On the other hand, because of data limitations, time scales >24 months may be unreliable (Guttman 1999). Given the inclusion within the study area of different climatic regions, particularly the arid Inland River Basin, where the data set included several zero or near zero precipitation values, 3-, 6-, 9-, and 12-month SPIs were selected as the index of drought frequency analysis. The calculated number of 3-, 6-, 9-, and 12-month moderate/severe/extreme droughts per century (abbreviated as NMD3/NSD3/NED3, NMD6/NSD6/NED6, NMD9/NSD9/NED9, NMD12/NSD12/NED12, respectively) are shown in Table 4 and mapped by a spatial interpolate method (see Figs. 5 and 6).

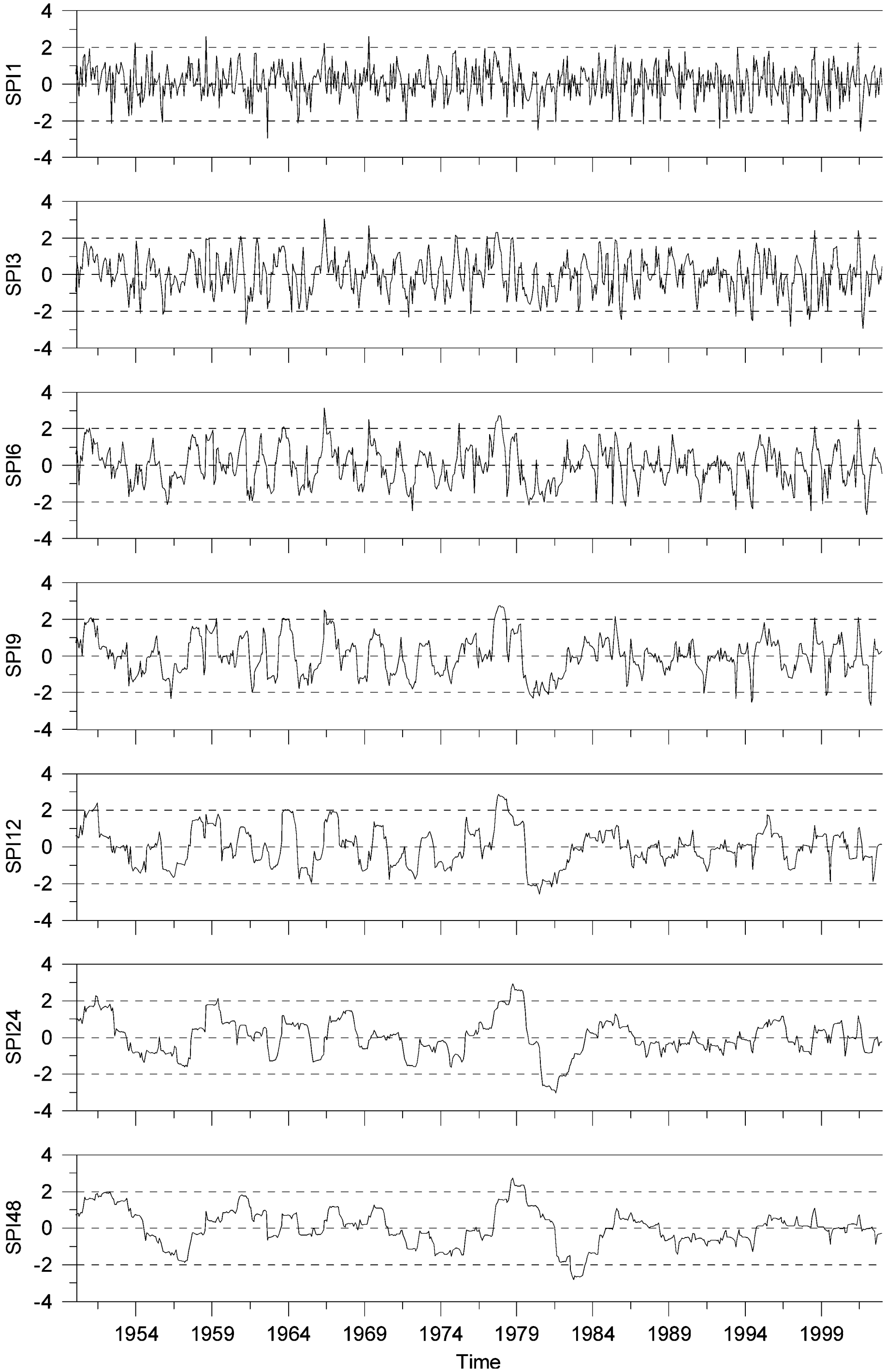

Fig. 3 SPI values for the Lanzhou station for the period from January 1951 to December 2003

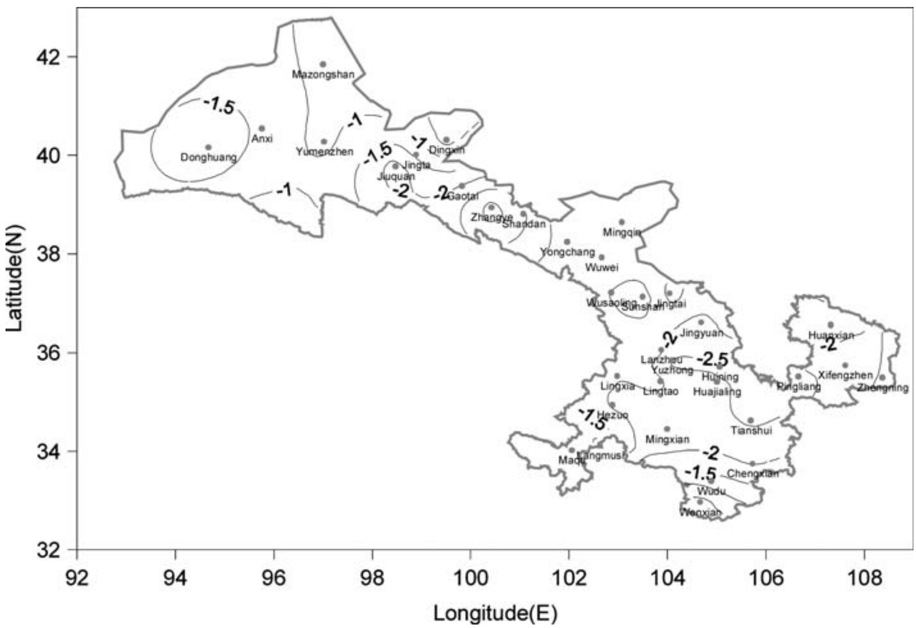

Fig. 4 Distribution of 6-month (January through June 1962) drought in Gansu Province

The mean numbers of 3-, 6-, 9-, and 12-month moderate droughts per century were 21.6, 17.3, 11.5 and 8.2, respectively, for the Inland River Basin (Table 4). The numbers of severe droughts and extreme droughts were 6.5, 7.7, 5.7, 4.2 and 2.6, 4.7, 3.5, 2.7, respectively. In the Yellow Basin and Yangtze River Basin, the numbers of the different severity of 3-month time scale droughts per century were significantly greater than those in the Inland River Basin. However, for other time scales, the numbers of drought events were approximately the same. The stations subject to a 3-month severe drought include the Shandan, Zhangye, Yongchang, and Wuwei stations in the Inland River Basin, and the Wusaoling, Mingxian, Langmusi, Tianshui, Zhengning, and Pingliang stations in the Yellow River Basin. For the 6-month time scale, the stations subject to severe droughts include the Jingta and Shandan stations in the Inland River Basin, and the Jingtai, Jingyuan, Maqu, Langmusi, Tianshui, and Zhengning stations in the Yellow River Basin. The stations likely to suffer 3-month extreme droughts were the Gaotai, Yongchang, Wuwei, and Shandan stations in the Inland River Basin, and the Linxia, Huajialing, and Huining stations in the Yellow River Basin. No significant differences in the frequency of severe drought were apparent in the Yangtze River Basin. These results are concordant with the frequency of droughts monitored in recent years (Yin et al. 2005). These results show that effect of short droughts in the Yellow River Basin and Yangtze River Basin was more severe than similar events in the Inland River Basin.

The per-century frequency of severe drought events is greater in the southeast than that in the northwest portion of the province. The Yangtze River Basin and some areas of the Yellow River Basin were subjected to severe drought events on 3-, 6-, 9-, and 12-month time scales (see Fig. 5). This region constitutes the mainly rain-fed agricultural area of Gansu Province, and frequent droughts result in reduced agricultural production, and even impact local residents' drinking water supply. Among different time scales, 3-month

Table 4 The number of drought events in 100 years of different time periods at different time scales[a]

Stations	Frequency of moderate drought				Frequency of severe drought				Frequency of extremely drought			
	NMD3	NMD6	NMD9	NMD12	NSD3	NSD6	NSD9	NSD12	NED3	NED6	NED9	NED12
Mazongshan	26.06	14.49	12.03	8.50	4.23	6.71	5.42	4.60	2.11	8.13	4.01	2.12
Donghuang	10.40	14.14	11.76	8.70	1.98	5.96	5.13	2.36	0.00	2.23	2.81	3.23
Anxi	7.36	20.31	11.50	9.40	5.52	7.08	6.57	3.85	0.00	2.46	3.29	3.08
Yumenzhen	15.92	19.49	13.22	8.80	5.10	8.63	6.18	5.76	1.27	3.83	2.13	1.60
Dingxin	14.57	19.27	10.20	8.15	1.99	5.98	5.54	4.49	1.99	2.99	4.66	3.00
Jingta	15.00	15.67	12.34	8.16	5.00	10.35	5.23	3.92	1.25	1.88	3.14	2.51
Jiuquan	25.59	17.82	10.94	9.51	5.69	7.36	5.86	4.04	0.47	4.51	2.22	1.19
Gaotai	32.50	18.18	11.51	8.79	4.38	6.90	6.69	5.34	3.13	7.21	3.77	2.83
Zhangye	24.54	18.46	10.88	10.02	11.66	9.23	7.80	4.93	4.29	5.85	3.49	2.16
Shandan	31.21	15.02	12.15	7.52	15.92	11.18	4.90	3.84	5.10	5.75	4.48	3.52
Yongchang	29.87	19.87	11.96	5.22	11.69	6.84	4.35	3.92	5.84	7.49	5.00	4.24
Wuwei	23.93	16.31	12.53	7.70	8.59	7.69	6.16	5.24	5.52	6.15	3.49	2.93
Mingqin	27.39	19.17	11.30	7.84	3.82	7.67	5.97	3.68	3.18	3.19	3.84	3.36
Wusaoling	34.97	17.85	10.06	7.09	19.02	9.23	5.34	4.78	8.59	5.54	4.93	3.85
Sunshan	43.30	15.54	11.07	7.79	12.37	8.29	4.15	3.64	9.28	6.22	4.15	2.60
Jingtai	22.30	18.31	10.86	8.83	7.43	10.17	7.69	5.77	9.46	3.73	3.17	2.21
Lanzhou	18.81	16.38	14.74	12.30	11.88	9.18	7.12	4.47	8.42	5.21	2.32	1.61
Jingyuan	20.00	18.83	12.24	8.94	11.22	11.49	6.53	5.26	7.32	2.69	3.10	1.71
Yuzhong	27.39	17.89	13.43	12.64	8.92	6.71	6.18	4.64	5.73	4.79	3.41	1.76
Lingxia	30.48	16.35	11.81	8.32	11.23	9.92	7.33	4.97	10.70	5.09	2.86	2.95
Lingtao	30.88	20.79	14.02	11.56	14.75	7.16	5.08	3.82	8.29	4.39	2.93	1.50
Huining	39.85	16.98	9.32	6.62	14.29	6.79	6.05	3.78	9.77	6.42	4.53	3.02
Huajialing	34.34	19.64	11.29	8.93	14.46	7.25	6.25	4.84	11.45	5.74	4.03	2.42
Huanxian	30.35	16.96	13.86	15.08	14.48	6.57	6.00	3.12	5.52	4.84	1.39	0.87

Table 4 continued

Stations	Frequency of moderate drought				Frequency of severe drought				Frequency of extremely drought			
	NMD3	NMD6	NMD9	NMD12	NSD3	NSD6	NSD9	NSD12	NED3	NED6	NED9	NED12
Pingliang	31.05	12.93	8.27	5.55	17.37	9.23	7.57	5.94	7.37	6.60	4.40	3.30
Xifengzhen	34.65	16.13	12.91	9.57	15.35	7.44	4.30	4.22	5.94	5.71	4.14	2.36
Maqu	42.61	20.52	10.50	7.88	15.65	10.48	9.33	7.44	4.35	3.49	1.17	0.44
Langmusi	46.81	16.58	9.29	9.92	20.21	12.83	7.50	3.75	5.32	4.28	4.64	2.95
Hezuo	40.85	17.31	11.79	9.03	14.09	8.83	7.08	5.84	9.15	5.30	3.30	2.12
Mingxian	25.85	14.91	11.42	8.94	19.02	9.54	4.89	4.90	8.29	6.85	4.24	2.20
Wudu	25.77	15.39	13.35	12.64	17.79	9.23	4.93	3.24	8.59	5.54	3.08	1.85
Tianshui	40.59	15.39	11.09	9.57	19.80	10.67	8.61	6.83	7.43	5.21	2.98	1.86
Chengxian	36.77	19.93	15.27	11.46	16.18	9.59	6.90	5.36	9.56	5.17	1.72	1.29
Zhengning	36.84	19.25	13.35	10.02	18.05	10.57	8.06	6.99	9.02	4.53	2.27	0.95
Wenxian	26.15	16.60	13.40	7.93	16.92	5.41	4.64	5.22	8.46	7.72	3.09	2.32

[a] NMD: number of moderate droughts in 100 years; NSD: number of severe droughts in 100 years; NED: number of extreme droughts in 100 years

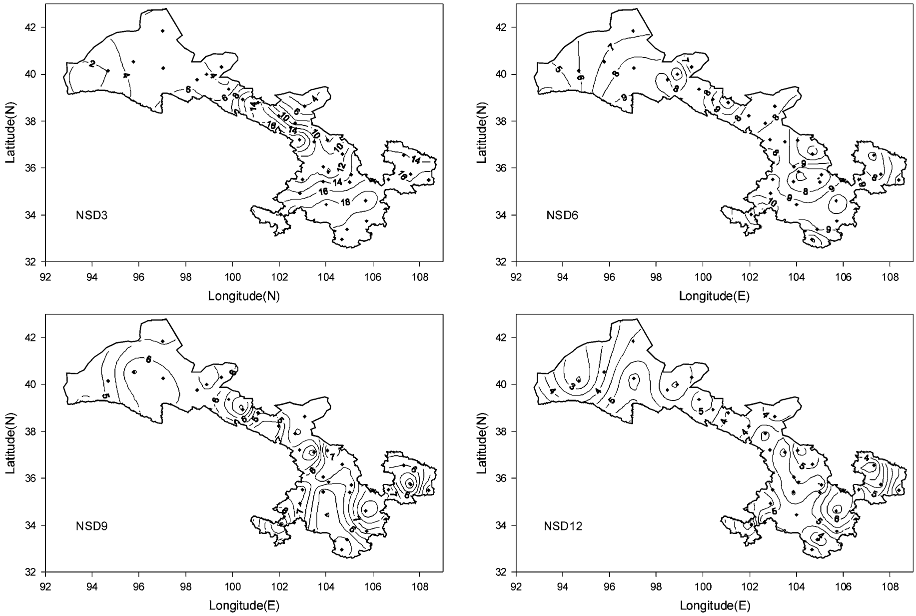

Fig. 5 Distribution of NSD3-12 (Number of severe drought in 100 years)

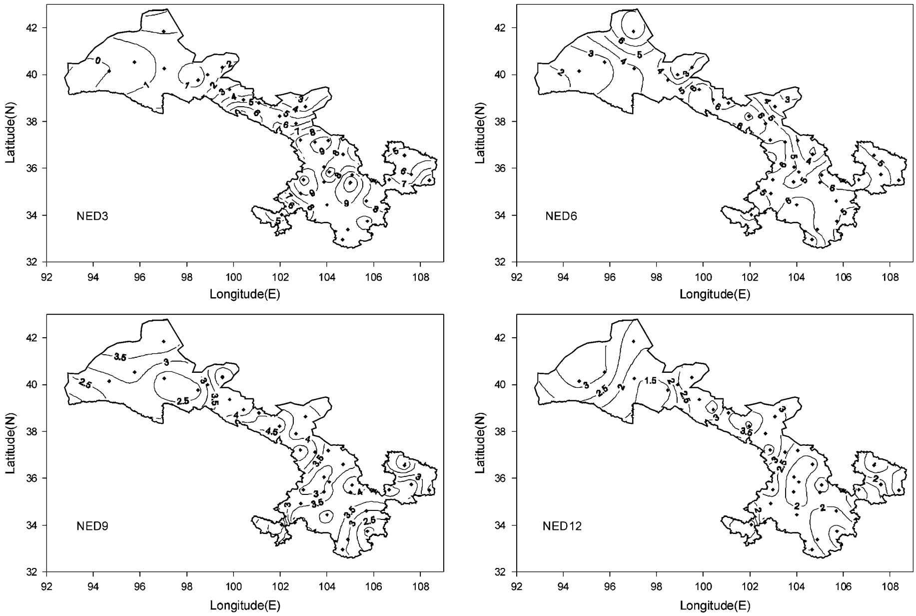

Fig. 6 Distribution of NED3-12 (Number of extreme drought in 100 years)

extreme drought events (NED3) occurred mainly in the Yellow River Basin and Yangtze River Basin (see Fig. 6), with nine such events per century, i.e., a devastating drought nearly every 10 years. The 6- and 9-month extreme droughts (NED6, NED9) extend to the majority of the province, except in the western portion of Inland River Basin. Conversely, the peak number of 12-month extreme droughts (NED12) per century occurred in the eastern and western portions of the Inland River Basin. This situation would have mainly affected ecosystems in the Hexi Corridor, and would have had less effect on the region's agriculture since farm irrigation is mainly dependent on the runoff from Qiliang Mountain.

Figure 5 shows that the frequency of severe drought (number of droughts in 100 years) in the southeast part of the province was greater than that in the northwest part. The Yangtze River Basin and some areas of the Yellow River Basin were subjected to severe drought at 3-, 6-, 9-, and 12-month time scales. This region is mainly the rain-fed agricultural area in Gansu Province, and frequent droughts result in the reduction of agriculture, and even impact the drinking water supply for local people. For different time scales, 3-month extreme drought (NED3) (see Fig. 6) mainly occurred in the Yellow River Basin and the Yangtze River Basin, amounting to 10.2 extreme droughts in 100 years, which implies that there would be a devastating drought per 10 years. The 6- and 9-month extreme droughts (NED6, NED9) extend to majority of the province except the western part of the Inland River Basin. Conversely, the number of 12-month extreme droughts (NED12) in 100 years was located in the eastern and western parts of the Inland River Basin. This situation mainly affected the ecosystem of the Hexi Corridor, and had less effect on agriculture of the region where farm irrigation was mainly dependent on the runoff of the Qiliang Mountain.

From Table 4, it is seen that the frequency of drought events for varying time periods is dramatically different. According to the SPI value and its cumulative probability of different drought events (Table 3), the frequency of drought for all time scales to a certain drought severity should be very close, and the frequency of the certain drought for all time scales approaches about 9.19, 4.4, and 2.28 for moderate, severe, and extreme drought, respectively. In this study, the dramatic difference between varying time periods is due to the short length of rainfall data sets at some points. The short sample size of precipitation leads to instability of the parameter estimates and the SPI calculated with this sample is likely not to capture the 'signals' of climate variability (Wu et al. 2005); however, this method can be utilized to approximately estimate the frequency of drought. On the other hand, modification of drought class criteria can allow calculated frequency of drought to be closer to the probability of SPI distribution.

4 Conclusion

The following conclusions can be drawn from the above analysis:

- The SPI is applicable to Gansu Province. A more flexible method and nominal SPI classification which is suitable to lower precipitations in arid and semi-arid regions would be needed in future studies.
- Water resources management strategies must be adjusted according to changing trends in rainfall and the spatial patterns of drought frequency. Most portions of Gansu Province receive little precipitation and show a downward trend in rainfall in specific months. For the most part of Gansu Province, such changes in precipitation are detrimental to agricultural production and ecosystem rehabilitation in arid and semi-arid regions. In particular, the southern region of the province requires a more efficient measurement of regulation to manage water resources and meet the requirements of agricultural and drinking water supply. The trend of precipitation in the arid Inland

River Basin will tend to accelerate desertification and increase the frequency of sandstorms in the future.

- More attention should be focused on precipitation trends and drought distribution during the agricultural development decision-making process and drought hazards mitigation. Increasingly rainy summers and drier fall-winter-spring seasons could result in summer water logging damage and insufficient spring soil moisture content.
- Short time drought has affected the Yellow River Basin and Yangtze River Basin more than the Inland River Basin. This situation mainly affects the urban and rural people's lives as well as the agricultural development of Gansu Province.
- Future studies need to investigate the specific effect of drought on sandstorms and the regional environment.

Acknowledgments This study was supported by the National Natural Science Foundation of China (Grant No. 40671010; 40725001). The authors greatly appreciate the help of the China Meteorological Data Sharing Service System (http://cdc.cma.gov.cn/) and the Hydrology and Water Resources Survey Administration of the Gansu Province for providing valuable pluviometric data. The authors also acknowledge the comments and advice from Dr. Chansheng He at the Department of Geography, Western Michigan University. We also thank two anonymous reviewers for providing constructive comments in reviewing this manuscript.

References

Abramowitz M, Stegun I (eds) (1965) Handbook of mathematical functions with formulas, graphs, and mathematical table. Dover Publications, New York

Chow V, Maidment R, Mays W (1988) Applied hydrology. McGraw-Hill, New York

Edwards D, McKee T (1997) Characteristics of 20th century drought in the United States at multiple scale. Atmospheric Science Paper No. 634, May 1–30

Guttman N (1998) Comparing the Palmer drought index and the standardized precipitation index. J Am Water Resour Assoc 34(1):113–121. doi:10.1111/j.1752-1688.1998.tb05964.x

Guttman N (1999) Accepting the standardized precipitation index: a calculation algorithm. J Am Water Resour Assoc 35(2):311–322. doi:10.1111/j.1752-1688.1999.tb03592.x

Hayes M, Svoboda M, Wilhite D et al (1999) Monitoring the 1996 drought using the standardized precipitation index. Bull Am Meteorol Soc 80:429–438. doi:10.1175/1520-0477(1999)080<0429:MTDUTS>2.0.CO;2

Hirsch R, Helsel D, Cohn T, Gilroy E (1993) Statistical analysis of hydrologic data. In: Maidment D (ed) Handbook of hydrology. McGraw-Hill, New York

Hisdal H, Stahl K, Tallaksen L et al (2001) Have streamflow droughts in Europe become more severe or frequent? Int J Climatol 21:317–333. doi:10.1002/joc.619

Husak G, Michaelsen J, Funk C (2007) Use of gamma distribution to represent monthly rainfall in Africa for drought monitoring applications. Int J Climatol 27:935–944. doi:10.1002/joc.1441

Kangas R, Brown T (2007) Characteristics of US drought and pluvials from a high-resolution spatial dataset. Int J Climatol 27:1303–1325. doi:10.1002/joc.1473

Łabędzki L (2007) Estimation of local drought frequency in central Poland using the Standardized Precipitation Index SPI. Irrig Drain 56:67–77. doi:10.1002/ird.285

Li Q, Liu X, Li X (2002) Drought trend in North in recent half century. J Nat Disasters 11(3):50–56 (in Chinese)

Li Y, Yu Y, Luo X, Ma X, Zhang A, Wang R (2004) Study on climatic prediction of sandstorm in east of Hexi Corridor. Plateau Meteorol 23(6):851–856 (in Chinese)

Ma Z, Dan L (2005) Dry/wet variation and its relationship with regional warming in arid regions of northern China. Chin J Geophys 48(5):1091–1099

Ma Z, Fu C (2006) Some evidence of drying trend over northern China from 1951 to 2004. Chin Sci Bull 51(23):2913–2925. doi:10.1007/s11434-006-2159-0

McKee T, Doesken N, Kleist J (1993) The relationship of drought frequency and duration to time scale. In: 8th conference on applied climatology, pp 179–184

Morid S, Smakhtin S, Moghaddasi M (2006) Comparison of seven meteorological indices for drought monitoring in Iran. Int J Climatol 26:971–985. doi:10.1002/joc.1264

Ntale H, Thian Y (2003) Drought indices and their application to East Africa. Int J Climatol 23:1335–1357. doi:10.1002/joc.931

Paulo A, Pereira L (2006) Drought concepts and characterization: comparing drought indices applied at local and regional scales. Water Int 31(1):37–49

Pereira L, Cordery I, Iacovides I (2002) Coping with water scarcity. UNESCO IHP VI, Technical Documents in Hydrology No. 58, UNESCO, Paris, p 269

Ren H, Zhang P, Li W, Gao L (2006) Low-frequency oscillation characteristics of precipitation and water vapor transport in the eastern part of Northwest China in spring. Plateau Meteorol 25(2):285–292 (in Chinese)

Salas J (1993) Analysis and modeling of hydrologic time series. In: Maidment D (ed) Handbook of hydrology. McGraw-Hill, New York, pp 19.1–19.72

Shi Y, Shen Y, Li D, Zhang G, Ding Y, Hu R, Kang E (2003) Discussion on the present climate change from warm-dry to warm-wet in northwest China. Quat Sci 23(2):152–164 (in Chinese)

Silva V (2005) On climate variability in Northeast of Brazil. J Arid Environ 58(4):575–596

Sneyers R (1990) On the statistical analysis of series of observations. WMO Technical Note 43, World Meteorological Organization, Geneva

Tate E, Gustard A (2000) Drought definition: a hydrological perspective. In: Vogt J, Somma F (eds) Drought and drought mitigation in Europe. Kluwer, Dordrecht, pp 23–48

Thom H (1966) Some methods of climatological analysis. WMO Technical Note Number 81, Secretariat of the World Meteorological Organization, Geneva, p 53

Wang Z, Zhai P (2003) Climate change in drought over northern China during 1950–2000. Acta Geogr Sin 58(Supplement):61–68 (in Chinese)

Wang Q, Ding Y, Jiang Y (1998) Relationship between Asian Monsoon activities and the precipitation over China mainland. Quat J Appl Meteorol 9(Supplement):84–89 (in Chinese)

Wilhite D, Glantz M (1985) Understanding the drought phenomenon: the role of definition. Water Int 10:111–120

Wu H, Hayes M, Weiss A, Hu Q (2001) An evaluation of the standardized precipitation index, the China-Z index and the statistical Z-Score. Int J Climatol 21:745–758. doi:10.1002/joc.658

Wu H, Hayes M, Wilhite D, Svoboda M (2005) The effect of the length of record on the standardized precipitation index calculation. Int J Climatol 25:505–520. doi:10.1002/joc.1142

Wu H, Svoboda M, Hayes M, Wilhite D, Wen F (2007) Appropriate application of the Standardized Precipitation Index in arid locations and dry seasons. Int J Climatol 27:65–79. doi:10.1002/joc.1371

Xu X, Tao S, Wang J, Chen L, Zhou L, Wang X (2002) The relationship between water vapor transport features of Tibetan Plateau-Monsoon "large triangle" affecting region and drought-flood abnormality of China. Acta Meteorol Sin 60(3):257–266 (in Chinese)

Yin X, Deng Z, Xu Q, Dong A (2005) Study on drought disasters in Gansu Province since recent 50 years. Arid Zone Res 22(1):120–124 (in Chinese)

Yu Y, Zou S, Whittemore D (1993) Non-parametric trend analysis of water quality data of rivers in Kansas. J Hydrol (Amst) 150:61–80. doi:10.1016/0022-1694(93)90156-4

Zhang Q (1998) Research on determination of drought index in north China and its application. J Catastrophol 13(4):34–38 (in Chinese)

Zhang Q, Chen L (1991) Variations of dryness and wetness in China during 1951–1980. Sci Atmos Sin 15(5):72–81 (in Chinese)

Zhang Q, Wei J, Tao S (2003) The decadal and interannual variations of drought in the northern China and association with the circulation. Clim Environ Res 8(3):307–318 (in Chinese)